Input Impedance and Resonant Frequency of a Printed Dipole With Arbitrary Length Embedded in Stratified Uniaxial Anisotropic Dielectrics

Benjamin D. Braaten, *Graduate Student Member, IEEE*, Robert M. Nelson, *Senior Member, IEEE*, and David A. Rogers, *Life Member, IEEE*

***Abstract*—Spectral domain immittance functions based on Hertz vector potentials are used to study the characteristics of a printed dipole with an arbitrary length embedded in stratified uniaxially anisotropic dielectrics. In particular, the resonant frequency and input impedance of the printed dipole are determined for various dielectric properties and thicknesses. Several newly computed results are compared to measurements, published literature, and commercial software for validation and are shown to have good agreement in all cases.**

***Index Terms*—Printed dipole, spectral domain immittance functions, uniaxial anisotropic dielectrics.**

I. Introduction

THE study of printed antennas in the presence of stratified anisotropic material has received considerable attention in the past [1]–[9]. This is because it is well known that many microwave substrates actually possess anisotropic properties [10]. The anisotropy ratio of the material can affect the input impedance [2], resonant frequency, [5] and far-field radiation pattern [1], [9] of an antenna. In particular, because of their resonant nature, printed dipoles are very sensitive to the anisotropy ratio of a substrate. Because of this resonant characteristic, it is very important to be able to model the printed dipole and the surrounding environment with accuracy, especially for radio frequency identification (RFID) applications [11]. Previous work has been done to model printed dipoles in isotropic dielectrics [11]–[13] as well as the radiation pattern and input impedance in the presence of stratified anisotropic dielectrics [9], [14].

In much of the research associated with anisotropic material, the dipole is assumed to be Hertzian, or a certain current distribution is assumed [14]. Many times, these assumptions about the current are not sufficient [12]. By not assuming a current distribution, the number of printed dipole problems that can be studied goes from a few special cases to a much larger number of more general problems. Extending to more general problems will be very useful to some of the recent research associated with printed dipoles [15], [16].

This work extends previous printed dipole research by studying the characteristics of a printed dipole of arbitrary length embedded in a structure of stratified uniaxial anisotropic dielectrics. The current distribution cannot be assumed in this work because the length of the printed dipole and the anisotropic layer properties are arbitrary. The current distribution is determined by applying the moment method to the spectral domain immittance functions found in [5]–[7]. Solving for the current on the printed dipole will directly show how each individual component of the anisotropic permittivity of each layer affects the characteristics of the printed dipole. In particular, this letter investigates how the anisotropic layers affect the resonant frequency and input impedance of the printed dipole. This will lead to new and useful information about how to incorporate the individual components of the anisotropic permittivity in a design of a printed dipole. An immediate and useful application of the results presented in this letter would be to study the process of using a printed antenna in a hybrid multilayered printed circuit board [17].

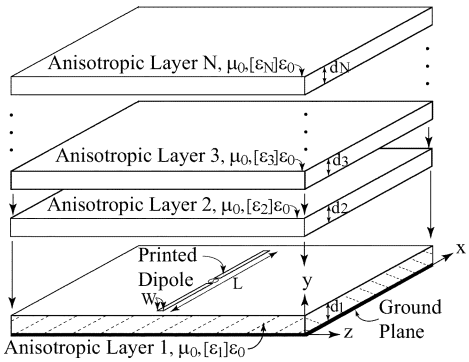

Fig. 1. Expanded view of the printed dipole in N layers of anisotropic material.

II. Problem Definition and the Spectral Domain Immittance Functions

The problem in Fig. 1 will be used to determine how the printed dipole is affected by the anisotropic layers. This structure consists of N layers of anisotropic dielectrics, extending to infinity in the x- and z-directions, with a printed dipole on layer 1. It is assumed that each layer has an optical axis in the y-direction, and the kth layer has a thickness of d_k and a permeability of μ_0 and is uniaxially anisotropic with permittivity $[\varepsilon_k]$. The dipole on layer 1 has a length L and width W and is

Manuscript received March 05, 2009; revised April 15, 2009. First published May 05, 2009; current version published July 28, 2009.

B. D. Braaten and D. A. Rogers are with the Department of Electrical and Computer Engineering, North Dakota State University, Fargo, ND 58102 USA (e-mail: benbraaten@ieee.org; d.a.rogers@ieee.org).

R. M. Nelson is with the Engineering and Technology Department, University of Wisconsin-Stout, Menomonie, WI 54751 USA (e-mail: r.m.nelson@ieee.org).

Color versions of one or more of the figures in this letter are available online at http://ieeexplore.ieee.org.

Digital Object Identifier 10.1109/LAWP.2009.2021992

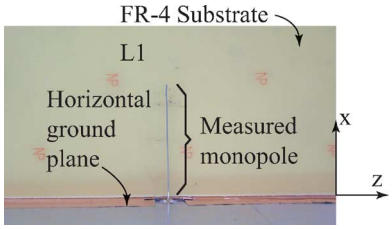

Fig. 2. Monopole used for testing on FR-4 substrate for single-layer problem.

driven with a delta source at the origin and assumed to be a thin wire. Thus, it is understood that the current does not vary with respect to the width of the conductor. This then requires only the tangential component of the electric field in the *x*-direction to be enforced to satisfy the tangential boundary conditions.

Next, the following expression [5]–[7] is used to solve for the currents on the printed dipoles:

$$\widetilde{E}_{x2}(\alpha, y, \beta) = \widetilde{J}_{xi}\widetilde{Z}_{xxi} \tag{1}$$

where $i = 1$ or 2, $\widetilde{E}_{x2}(\alpha, y, \beta)$ represents the electric field in region 2, and $\widetilde{Z}_{xxi}$ is referred to as the spectral domain immittance function. $\widetilde{J}_{x1}$ (i = 1) was chosen to represent an *x*-directed dipole current on layer 1, or $\widetilde{J}_{x2}$ (i = 2) was chosen to represent an *x*-directed dipole current on layer 2. The spectral domain moment method [18] is used to solve for the unknown currents $\widetilde{J}_{xi}$. The steps leading to (1) are quite extensive and are beyond the scope of this letter. A thorough derivation of $\widetilde{Z}_{xxi}$ can be found in [5]–[7]. In sections that follow, N has a value of three or less.

III. Measurement and Numerical Results

A. Measurement Validation

Advanced Design System (ADS) [19] was used as a tool throughout this work to validate the calculations by the immittance functions for the isotropic problems. Thus, the first step was to validate the results from the immittance functions and ADS with measurements. To do this, a wire dipole similar to the one presented in [12] was placed above a 1.58-mm grounded substrate made of FR-4 material. The wire dipole had a radius of $a = 0.4$ mm and length $L = 60$ mm, and it was assumed that the FR-4 material had a permittivity of 4.35. The grounded FR-4 substrate and dipole were placed vertically above a ground plane and driven through a coaxial line. This setup is shown in Fig. 2. The resonant frequency was measured with a calibrated Agilent E5071C ENA series network analyzer for various isotropic and anisotropic superstrates of one and two layers. An equivalent problem of a flat printed dipole with the same length and width of $W = 4\mathrm{a}$ was defined to be evaluated by ADS and the immittance functions. It has been shown that a flat printed "strip" conductor with a width of $W = 4\mathrm{a}$ can be used to approximate a thin wire cylindrical conductor with radius a [20]. Two-dimensional piecewise sinusoidal (PWS) functions similar to the ones used in [12] were used as basis functions, except that the PWS functions were constant in the z-direction and the same width as the dipole. The limit of integration was $500k_0$.

The results from these measurements and simulations are shown in Table I. Layer 1 (L1) refers to the substrate, layer 2 (L2) refers to the superstrate immediately above the monopole (i.e., superstrate touching the monopole), and layer 3 (L3) refers to the superstrate above layer 2 (i.e., the superstrate between layer 2 and the surrounding air). The Epsilam-10 (E-10) material has a thickness of 0.635 mm with $\varepsilon_x = 13.0$ and $\varepsilon_y = 10.2$. The Rogers RT/Duroid 5880 has a thickness of 0.7874 mm and $\varepsilon = 2.2$. Table I shows good agreement between the measurements and numerical results from the spectral domain immittance functions and ADS. These measurements illustrate that the immittance functions are accurately calculating various properties of the printed dipole with isotropic and anisotropic layers and that ADS can be used as a good tool to validate the isotropic results.

TABLE I
Measured Resonant Frequency of a Monopole in Layered Material

L1	L2	L3	ADS	Equation (1)	Measured
FR-4	Air	Air	704 MHz	704 MHz	706 MHz
FR-4	FR-4	Air	615 MHz	615 MHz	617 MHz
FR-4	5880	Air	673 MHz	674 MHz	676 MHz
FR-4	E-10	Air	X	564 MHz	566 MHz
FR-4	E-10	5880	X	555 MHz	554 MHz
FR-4	E-10	FR-4	X	539 MHz	540 MHz

B. Further Microstrip Resonator Validation

It should also be mentioned that extensive computations were performed involving a microstrip resonator emersed in one-, two-, and three-layer anisotropic structures. The results from these computations were successfully compared to the published results in [5], [21], and [22]. This provided further validation that the computations in this work are accurate for both the isotropic and anisotropic structures.

C. Single-Layer Problem ($N = 1$)

For the single-layer problem, the printed dipole in Fig. 1 was evaluated by the spectral domain immittance functions with $d_2 = d_3 = 0$. In particular, the resonant frequency and input impedance were determined for various values of d_1 and anisotropy ratios. First, an anisotropic dielectric was defined in region 1. The anisotropy ratio was varied in both directions, while the thickness was set at 1.58 mm. Initially, ε_{y1} ($\varepsilon_{y1} = \varepsilon_{11}$) was varied while ε_{x1} ($\varepsilon_{x1} = \varepsilon_{12}$) was set to 2.55. Then, ε_{x1} was varied while ε_{y1} was set to 2.55. The resonant frequency results for these sweeps are shown in Fig. 3(a), where it is shown that the isotropic case corresponds well with the results from ADS. Finally, an anisotropic substrate of boron nitride ($\varepsilon_y = 3.14$, $\varepsilon_x = 5.12$), sapphire ($\varepsilon_y = 11.6$, $\varepsilon_x = 9.4$) and Epsilam-10 ($\varepsilon_y = 10.2$, $\varepsilon_x = 13$) was defined, and the resonant frequency of the dipole was calculated as the thickness of the substrate was increased. The results are shown in Fig. 3(b).

It is shown in Fig. 3 that the resonant frequency decreases significantly as the value of the permittivity is increased, while a change in thickness has only a small effect on the resonant frequency. In particular, the resonant frequency is mainly affected by the *y*-component of $[\varepsilon_1]$. This is because the dominant TM_0 mode is present, which has a field component in the substrate in the *y*-direction [1]. Thus ε_{y1} is not increasing the substrate effective thickness, but it is increasing the effective length of the dipole.

The next problem extended the isotropic results by Rana and Alexopoulos [12] to include an anisotropic substrate. Rana and

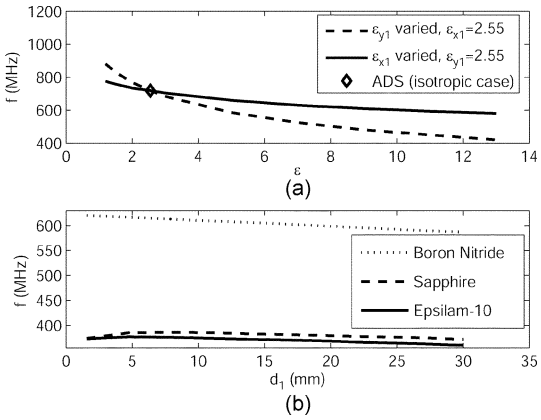

Fig. 3. Resonant frequency of a printed dipole on a single anisotropic substrate with various values of (a) $[\varepsilon_1]$ and (b) boron nitride, sapphire, and Epsilam-10 substrates.

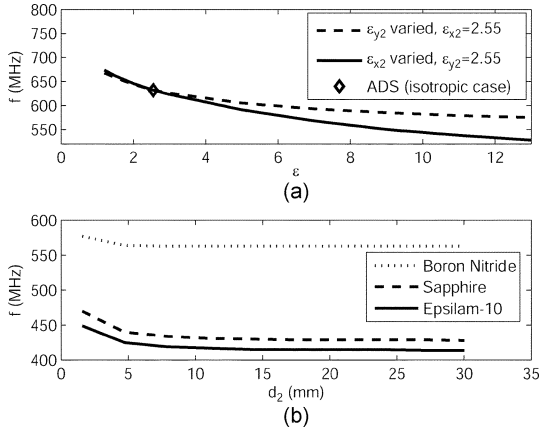

Fig. 5. Resonant frequency of a printed dipole with an anisotropic superstrate with (a) various values of ε_{y2} and ε_{x2} and (b) various thicknesses of boron nitride, sapphire, and Epsilam-10.

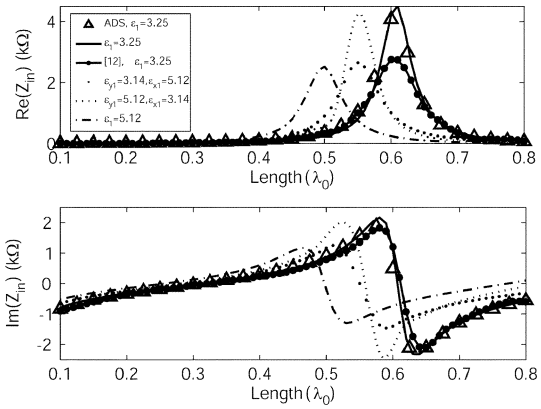

Fig. 4. Computed input impedance of the printed dipole on a single anisotropic layer.

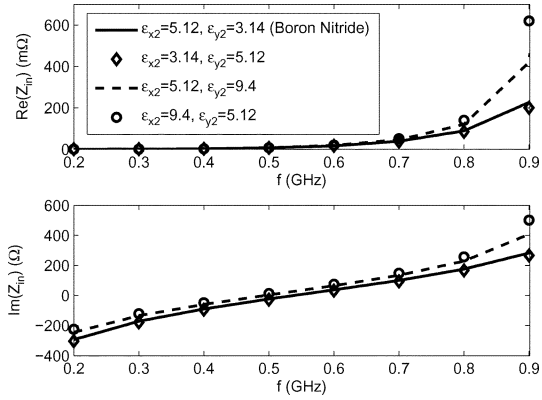

Fig. 6. Computed input impedance of the printed dipole in two anisotropic layers for various values of $[\varepsilon_2]$.

Alexopoulos calculated the input impedance for various lengths of a printed dipole with a single isotropic substrate. Instead of the printed dipole defined in Fig. 1, Rana and Alexopoulos defined a thin wire dipole with radius $\mathrm{a} = 0.0001\lambda_0$ on a substrate with thickness $d_1 = 0.1016\lambda_0$ and $\varepsilon_r = 3.25$. Again, a flat printed "strip" conductor with a width of $W = 4\mathrm{a}$ was evaluated by the immittance functions and ADS. The isotropic results computed by the immittance functions are shown to compare well to the results from ADS and the results by Rana and Alexopoulos in Fig. 4. Several anisotropic results are also shown in Fig. 4. It was shown that the resonant length of the antenna is influenced mainly by the component of the permittivity in the direction of the optical axis. This corresponds to the results in Fig. 3.

D. Two-Layer Problem $(N = 2)$

A two-layer problem for a printed dipole with an anisotropic superstrate $(\mathrm{N} = 2)$ was considered next. Again, the printed dipole in Fig. 1 was placed at $y = d_1$ and was defined to have a length of 15 cm and a width W of 0.5 mm. An anisotropic superstrate was defined for region 2, and $[\varepsilon_2]$ was varied in region 2. The computed resonant frequency for the dipole is shown in Fig. 5(a) for $\varepsilon_1 = 2.55$ and $d_1 = 1.58$ mm. Notice that the isotropic case agrees well with the results from ADS. Next, region 2 was replaced by various anisotropic materials: boron nitride ($\varepsilon_{x2} = 5.12$ and $\varepsilon_{y2} = 3.14$), sapphire ($\varepsilon_{x2} = 9.4$ and $\varepsilon_{y2} = 11.6$), and Epsilam-10 ($\varepsilon_{x2} = 13$ and $\varepsilon_{y2} = 10.2$). The thickness of region 2 was increased, and the resonant frequency was calculated. The results are shown in Fig. 5(b) for $\varepsilon_1 = 2.55$ and $d_1 = 1.58$ mm. Next, the input impedance of the printed dipole was computed for various values of $[\varepsilon_2]$. These results are shown in Fig. 6 for $\varepsilon_1 = 3.25$ and $d_1 = 1.58$ mm.

The effect that layer 2 has on the resonant frequency of the dipole is related to the space-waves and surface modes launched from the dipole. For a layer thickness of 1.58 mm, it can be assumed that only the TM_0 is present in the surface wave [12]. For this case, the electric field has the strongest component along the axis of the dipole with a component orthogonal to the direction of propagation in a position broadside to the dipole. In all these cases, the electric field has a component in the x-z plane that corresponds to the greater effect caused by ε_{x2} and ε_{z2} and not by ε_{y2}. Finally, as the thickness of layer 2 is increased, the effect on the resonant frequency is reduced.

E. Three-Layer Problem $(N = 3)$

The next structure evaluated was the printed dipole in a three-layer structure. Here, the printed dipole was moved from on top

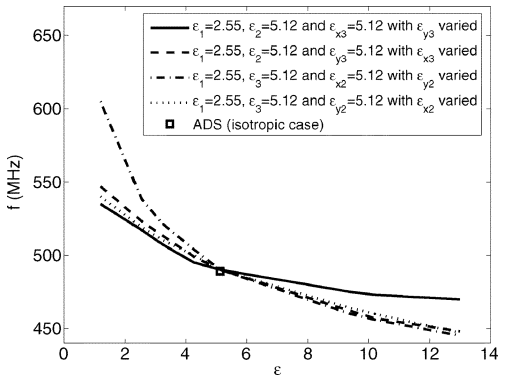

Fig. 7. Resonant frequency of a printed dipole in three layers with various values of $[\varepsilon_2]$ and $[\varepsilon_3]$.

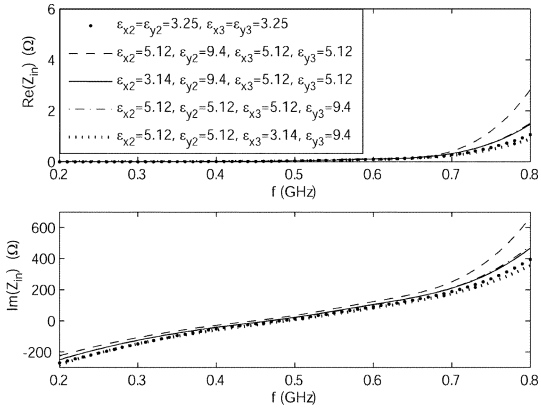

Fig. 8. Computed input impedance of the printed dipole in three anisotropic layers for various values of $[\varepsilon_2]$ and $[\varepsilon_3]$.

of layer 1 to on top of layer 2. The depth of each of the three layers was set at 1.58 mm, and the dipole had a length of 15 cm and a width of 0.5 mm. The isotropic layer next to the ground plane (layer 1) had a permittivity of $\varepsilon_1 = 2.55$. The values of $[\varepsilon_2]$ and $[\varepsilon_3]$ were varied, and the computational results for these cases are shown in Fig. 7. Finally, the input impedance of the printed dipole was computed for various values of $[\varepsilon_2]$ and $[\varepsilon_3]$. These results are shown in Fig. 8 for $\varepsilon_1 = 3.25$. Finally, it should be mentioned that the isotropic results in Fig. 8 were successfully validated with ADS.

IV. Discussion

Several important comments can be made about the results in Figs. 3–8.

1) In Figs. 3(a), 5(a), and 7, it is shown that the permittivity in the direction of the optical axis in the layers below the printed dipole has the most impact on the resonant frequency as opposed to the permittivity in the direction orthogonal to the optical axis.
2) When considering the resonant frequency effects (Figs. 5(a) and 7) of an anisotropic layer above the printed dipole, it is shown that the permittivity in the direction orthogonal to the optical axis is dominant.
3) From the results in Figs. 3(b) and 5(b), it can be concluded that as the thickness of the anisotropic layers is increased, the effect on the resonant frequency is significantly reduced.
4) When considering the radiation resistance in Figs. 4 and 8, it is shown that the largest radiation resistance values in the anisotropic results are associated with the larger values of permittivity in the direction of the optical axis in the layers below the dipole.
5) When considering the radiation resistance in Fig. 6, it is shown that the largest radiation resistance values in the anisotropic results are associated with the larger values of permittivity orthogonal to the optical axis in the layers above the dipole.

V. Conclusion

A printed dipole of arbitrary length embedded in several anisotropic layers was investigated using the spectral domain immittance method. Original numerical results were validated by comparison with measurements, published literature, and commercial software. By not assuming a current distribution, the new results in this letter have clearly shown how each component of the permittivity in each layer can affect the resonant frequency and input impedance of a printed dipole with arbitrary length.

References

[1] D. M. Pozar, "Radiation and scattering from a microstrip patch on a uniaxial substrate," *IEEE Trans. Antennas Propag.*, vol. AP-35, no. 6, pp. 613–621, Jun. 1987.
[2] J. R. S. Oliveira and A. G. D'Assuncao, "Input impedance of microstrip patch antennas on anisotropic dielectric substrates," in *Proc. IEEE Antennas Propag. Soc. Int. Symp. Dig.*, Jul. 21–26, 1996, pp. 1066–1069.
[3] C. S. Gurel and E. Yazgan, "Characteristics of a circular patch microstrip antenna on uniaxially anisotropic substrate," *IEEE Trans. Antennas Propag.*, vol. 52, no. 10, pp. 2532–2537, Oct. 2004.
[4] V. Losada, R. R. Boix, and M. Horno, "Full-wave analysis of circular microstrip resonators in multilayered media containing uniaxial anisotropic dielectrics, magnetized ferrites, and chiral materials," *IEEE Trans. Microw. Theory Tech.*, vol. 48, no. 6, pp. 1057–1064, Jun. 2000.
[5] R. M. Nelson, D. A. Rogers, and A. G. D'Assuncao, "Resonant frequency of a rectangular microstrip patch on several uniaxial substrates," *IEEE Trans. Antennas Propag.*, vol. 38, no. 7, pp. 973–981, Jul. 1990.
[6] H. Lee and V. K. Tripathi, "Spectral domain analysis of frequency dependent propagation characteristics of planar structures on uniaxial medium," *IEEE Trans. Microw. Theory Tech.*, vol. MTT-30, no. 8, pp. 1188–1193, Aug. 1982.
[7] T. Itoh, "Spectral domain immitance approach for dispersion characteristics of generalized printed transmission lines," *IEEE Trans. Antennas Propag.*, vol. AP-28, no. 7, pp. 733–736, Jul. 1980.
[8] F. L. Mesa, R. Marques, and M. Horno, "A general algorithm for computing the bidimensional spectral Green's dyad in multilayered complex bianisotropic media: The equivalent boundary method," *IEEE Trans. Microw. Theory Tech.*, vol. 39, no. 9, pp. 1640–1649, Sep. 1991.
[9] A. Eroglu and J. K. Lee, "Far field radiation from an arbitrarily orientated Hertzian dipole in the presence of layered anisotropic medium," *IEEE Trans. Antennas Propag.*, vol. 53, no. 12, pp. 3963–3973, Dec. 2005.
[10] N. G. Alexopoulus, "Integrated-circuit structures on anisotropic substrates," *IEEE Trans. Microw. Theory Tech.*, vol. MTT-33, no. 10, pp. 847–881, Oct. 1985.
[11] B. D. Braaten, G. J. Owen, D. Vaselaar, R. M. Nelson, C. Bauer-Reich, J. Glower, B. Morlock, M. Reich, and A. Reinholz, "A printed Rampart-line antenna with a dielectric superstrate for UHF RFID applications," in *Proc. IEEE Int. Conf. on RFID*, Las Vegas, NV, Apr. 16–17, 2008, pp. 74–80.

[12] I. E. Rana and N. G. Alexopoulos, "Current distribution and input impedance of printed dipoles," *IEEE Trans. Antennas Propag.*, vol. AP-29, no. 1, pp. 99–105, Jan. 1981.
[13] X. H. Wu, A. A. Kishk, and A. W. Glisson, "A transmission line method to compute the far-field radiation of arbitrarily directed Hertzian dipoles in a multilayer structure embedded with PEC strip interfaces," *IEEE Trans. Antennas Propag.*, vol. 55, no. 11, pp. 3191–3198, Nov. 2007.
[14] W. J. Wang, "Multilayered printed antennas with biaxial anisotropic dielectric substrates: General analysis and case studies," Ph.D. dissertation, Polytechnic Univ., Brooklyn, NY, Jan. 2002.
[15] A. Erentok, D. Lee, and R. W. Ziolkowski, "Numerical analysis of a printed dipole antenna integrated with a 3-D AMC block," *IEEE Antennas Wireless Propag. Lett.*, vol. 6, pp. 134–136, 2007.
[16] Y. Huang, A. De, Y. Zhang, T. K. Sarkar, and J. Carlo, "Enhancement of radiation along the ground plane from a horizontal dipole located close to it," *IEEE Antennas Wireless Propag. Lett.*, vol. 7, pp. 294–297, 2008.
[17] J. Broomall, T. Yost, and G. Walther, "Stripline performance in hybrid printed circuit boards," June 2005 [Online]. Available: www.circuitree.com
[18] D. B. Davidson and J. T. Aberle, "An introduction to the spectral domain method-of-moments formulations," *IEEE Antennas Propag. Mag.*, vol. 46, no. 3, pp. 11–19, Jun. 2004.
[19] Advanced Design System-ADS 2004A. Agilent Technologies.
[20] W. L. Stutzman and G. A. Thiele*, Antenna Theory and Design*, 2nd ed. New York: Wiley, 1998.
[21] T. Itoh and W. Menzel, "A full-wave analysis method for open microstrip structures," *IEEE Trans. Microw. Theory Tech.*, vol. MTT-29, no. 1, pp. 63–68, Jan. 1981.
[22] I. J. Bahl, P. Bhartia, and S. S. Stuchly, "Design of microstrip antennas covered with a dielectric layer," *IEEE Trans. Antennas Propag.*, vol. AP-30, no. 2, pp. 314–318, Mar. 1982.